



Detection of Water and Ice on Bridge Structures by AC Impedance and Dielectric Relaxation Spectroscopy Phase II

Final Report

Prepared by:

John F. Evans

Department of Chemistry and Biochemistry
University of Minnesota Duluth

Northland Advanced Transportation Systems Research Laboratories (NATSRL)
University of Minnesota Duluth

CTS 13-25

Technical Report Documentation Page

1. Report No. CTS 13-25	2.	3. Recipients Accession No.	
4. Title and Subtitle Detection of Water and Ice on Bridge Structures by AC Impedance and Dielectric Relaxation Spectroscopy Phase II		5. Report Date August 2013	
		6.	
7. Author(s) John F. Evans		8. Performing Organization Report No.	
9. Performing Organization Name and Address Department of Chemistry and Biochemistry University of Minnesota Duluth 1039 University Drive Duluth, Minnesota 55812		10. Project/Task/Work Unit No. CTS # 2009009 and 2010003	
		11. Contract (C) or Grant (G) No.	
12. Sponsoring Organization Name and Address Intelligent Transportation Systems Institute Center for Transportation Studies University of Minnesota 511 Washington Avenue SE, Suite 200 Minneapolis, Minnesota 55455		13. Type of Report and Period Covered Final Report 7/1/08 – 6/30/10	
		14. Sponsoring Agency Code	
15. Supplementary Notes http://www.its.umn.edu/Publications/ResearchReports/			
16. Abstract (Limit: 200 words) <p>During Phase I of this project, we have carried out preliminary evaluation of a novel approach to low-cost sensing systems for monitoring ice, water and deicing solutions on road bridge deck surfaces. Our initial approaches included the techniques of alternating current impedance and dielectric relaxation spectroscopy of responses from simple passive metal sensors. These preliminary results indicated that the second approach of dielectric relaxation spectroscopy was far more promising. Furthermore, likely implementations would be significantly more economical using lower-cost electronics modules connected to passive sensors.</p> <p>Our choice for implementation of dielectric relaxation spectroscopy is based on the measurement of high-frequency components of pulse waveforms reflected from the sensor and using time domain reflectometry (TDR). The information content of these waveforms is strongly influenced by the dielectric properties of the media of interest (ice, water or aqueous solutions of deicing chemicals) in contact with or in close proximity (microns) with passive metal conductors, which comprise the sensor.</p> <p>These high-frequency dielectric relaxation measurements using TDR probe the physical state of precipitation and deicing chemicals on the deck or road surface by the detailed examination of the frequency response waveforms returned after the application of a fast rise-time excitation pulse. Signal processing of the acquired waveforms involves taking the derivative of the response followed by digital filtering and subsequent wavelet analysis to emphasize and distinguished low vs high frequency components of the waveforms reflected from the sensors. Determination of the state and nature of the precipitation, solutions or air in contact with a given sensor is made on a statistical basis via correlation of responses to calibration waveforms collected under known conditions for a given sensor. The software to carry out these signal processing tasks in implemented using LabVIEW.</p>			
17. Document Analysis/Descriptors Snow and ice control, Sensors, Ice sensing, Snow sensing, Weather sensors, Safety		18. Availability Statement No restrictions. Document available from: National Technical Information Services, Alexandria, Virginia 22312	
19. Security Class (this report) Unclassified	20. Security Class (this page) Unclassified	21. No. of Pages 38	22. Price

Detection of Water and Ice on Bridge Structures by AC Impedance and Dielectric Relaxation Spectroscopy Phase II

Final Report

Prepared by:

John F. Evans

Department of Chemistry and Biochemistry
University of Minnesota Duluth

Northland Advanced Transportation Systems Research Laboratories (NATSRL)
University of Minnesota Duluth

August 2013

Published by:

Intelligent Transportation Systems Institute
Center for Transportation Studies
University of Minnesota
511 Washington Avenue SE, Suite 200
Minneapolis, Minnesota 55455

The contents of this report reflect the views of the authors, who are responsible for the facts and the accuracy of the information presented herein. This document is disseminated under the sponsorship of the Department of Transportation University Transportation Centers Program, in the interest of information exchange. The U.S. Government assumes no liability for the contents or use thereof. This report does not necessarily reflect the official views or policies of the Northland Advanced Transportation Systems Research Laboratories, the Intelligent Transportation Systems Institute or the University of Minnesota.

The authors, the Northland Advanced Transportation Systems Research Laboratories, the Intelligent Transportation Systems Institute, the University of Minnesota and the U.S. Government do not endorse products or manufacturers. Trade or manufacturers' names appear herein solely because they are considered essential to this report.

Acknowledgements

The author(s) wish to acknowledge those who made this research possible. The study was funded by the Intelligent Transportation Systems (ITS) Institute, a program of the University of Minnesota's Center for Transportation Studies (CTS). Financial support was provided by the United States Department of Transportation's Research and Innovative Technologies Administration (RITA).

The project was also supported by the Northland Advanced Transportation Systems Research Laboratories (NATSRL), a cooperative research program of the Minnesota Department of Transportation, the ITS Institute, and the University of Minnesota Duluth College of Science and Engineering.

The assistance of Mr. Evan Anderson and Mr. Luke Busta in the execution of this research project is gratefully acknowledged

Table of Contents

Chapter 1: Task Specifications	1
Chapter 2: Introduction	3
Chapter 3: Technical Background	5
Chapter 4: Development Focus and Sub-Tasks	9
Chapter 5: Sensor Test Stand.....	11
Chapter 6: Sensor Development and Refinement.....	13
Chapter 7: Acquisition and Testing of Commercial Electronic Components.....	19
Chapter 8: Software Development and Refinement	21
Chapter 9: System Integration and Testing.....	25
Chapter10: Suggestions for Future Work	27
References.....	29

List of Figures

Figure 3.1: Voltage vs time at a point on an impedance mismatched transmission line driven with a step voltage of height E_i	6
Figure 3.2: Transmission line with 6 dielectric discontinuities.	6
Figure 3.3: Idealized TDR trace for a series RC terminated transmission line.	7
Figure 5.1: Block diagram of temperature controlled test cell.	11
Figure 6.1: Machined Sensor, 0.25" square aluminum hot electrode and a 1.0" aluminum U-channel ground electrode with a 0.125" electrode gap.....	13
Figure 6.2: Coaxial sensor constructed from stainless steel vacuum feedthroughs	13
Figure 6.3: Linear sensor with small electrode gaps, 3"x0.5"x0.020" copper sheets with a 0.050" gap potted in a two part epoxy. Inner electrode is hot and outer two electrodes are ground.....	14
Figure 6.4: Linear sensor with large electrode gaps, 0.020"x0.5"x3" copper sheets with a 3/8" gap potted in a two part epoxy. Inner electrode is hot and outer two electrodes are ground.....	14
Figure 6.5: Jelly roll sensor, 0.020" copper sheet wound twice with a 1.0" outside diameter and potted in a two part epoxy. Hot and ground electrodes run side-by-side.	14
Figure 6.6: Open ring sensor with gaps in the diameter of the electrodes, 10 gauge copper wire with a ground electrode diameter of 1.125" and hot electrode diameter of 0.75" potted in a two part epoxy.....	14
Figure 6.7: Closed rings sensor, 10 gauge copper wire with a ground electrode diameter of 1.125" and hot electrode diameter of 0.75" potted in a two part epoxy.	14
Figure 6.8: Cone sensor, 12 gauge magnet wire wound three times with a diameter decreasing from 1.5" to 1.0" potted in a two part epoxy. Hot and ground electrodes run side-by-side.	15
Figure 6.9 Spiral sensor, 12 gauge magnet wire hot electrode wound three times around a 7/8" diameter copper pipe ground electrode and potted in a two part epoxy. (Pictured before potting).	15
Figure 6.10: Spiral sensor, 12 gauge magnet wire wound three times around a 0.020"x1.0"x4.0" copper ground electrode.....	15
Figure 6.11: Machined aluminum sensor which allows for variable thicknesses of dielectric to be sandwiched between the electrodes. Teflon dielectric shown.	15
Figure 6.12: Single threaded sensor, 3.5" threaded stainless steel hot electrode in an aluminum U-channel ground. Packing tape used in-between the electrodes as the dielectric.....	15
Figure 6.13: Mesh sensor, 3.0" long 12 gauge magnet wire over a 4x4 stainless steel mesh ground.	16

Figure 6.14: Example of poor raw data from a candidate sensor. Left to right: air, ice, frozen 0.1M NaCl, and water	16
Figure 6.15: Example of raw data with high complexity and information content. Left to right: air, ice, frozen 0.1M NaCl, and water	17
Figure 6.16: Raw responses for the sensor shown in Figure 6.2 for ice, air and water.	18
Figure 7.1: Schematic of a bridge deck installation at a remote location with 8 sensors deployed	19
Figure 8.1 Raw data file taken with TDR 7.5cm probe in air	22
Figure 8.2: Raw derivative of Fig. 8.1 showing increased information content and complexity. .	22
Figure 8.3: Savitzky-Golay smoothed derivative of Fig. 8.1.....	23
Figure 8.4: The waveform processing procedure implemented to optimize differentiability among waveforms, and the peak alignment technique used to overcome shifts induced by varying propagation rates due to changes in transmission line temperature	24
Figure 9.1: Freeze-thaw cycle for water from “remote” sensor located in the test stand. Raw data acquired by the datalogger transmitted to a “central” processing station running in-house developed software (written in LabVIEW).....	25

List of Tables

Table 6.1: Ideal sensor response.....	17
Table 6.2: Correlation coefficients for the sensor shown in Figure 6.2.....	18

Executive Summary

Proof of concept has been shown for the application of time domain reflectometry to the detection of air, water, ice and electrolyte in both liquid and frozen states in contact with passive metal transmission line sensors. Further work has been carried out to perfect the hardware and software required to make this economical transmission line technology practicable for deployment on bridge decks and other areas of concern, so that activation of safety signage or signaling to maintenance personnel can be automated based on the response of these sensor systems to unsafe road conditions (e.g., accumulation of ice, frost, etc.).

Chapter 1

Task Specifications

This report covers FY 2009 and FY 2010. As such, the tasks listed in the original proposals are listed below, and will be cross-referenced in the following chapters which describe the evolution of sensor, system, and software development.

FY 2009

1. Continued refinement of TDR parameters obtained for coaxial and parallel plate test cells constructed during year 1 of the project. Water, ice, electrolyte and air to be employed as media in cells. Definition of minimal requirements for reduced cost electronics package. *See Chapters 6-8*
2. Consultation with soil moisture TDR system vendors, and communication cable testing manufacturers to define system specifications and availability. Order appropriate system. *See Chapter 7*
3. Develop software for low-cost system. *See Chapter 8*
4. Carry out TDR measurements as in 1, above, using low-cost system. *See Chapter 9*
5. Prepare final report on suitability of low-cost multiplexed system. *This Document*

FY 2010

1. Continued refinement of TDR sensor design. Dimensions will be reduced, and coaxial and spiral transmission line terminations will be investigated. *See Chapter 6*
2. Implementation of multiplexed electronics system with integrated software compatible with sensor responses from task 1. *See Chapters 6-7*
3. Deploy system on an outdoor concrete pad test bed. *Deferred to Phase III*
4. Carry out TDR measurements using outdoor test bed during winter of 2009-10 *Deferred to Phase III*
5. Prepare final report on suitability of low-cost multiplexed system. *This Document*

Chapter 2

Introduction

Our research objective, simply stated, has been to develop reliable, low-cost water/ice sensors systems which can be deployed in a variety of critical locations. Our aim is to develop these technologies in configurations amenable to inclusion in remote sensing networks.

In light of the lack of affordable alternative ice/water detection systems, if we are successful, these outcomes could provide revolutionary sensing alternatives to those currently available. The benefits could be enormous in terms of decreasing loss of life, personal injury and loss of property at critical sites by virtue of making real time data available to trigger automated dispensing systems, or alert maintenance crews of immediate need for application of deicing chemicals to these critical areas. The primary benefits would accrue to the public in terms of reduced accident risk at critical traffic sites.

Chapter 3

Technical Background

Time Domain Reflectometry. Time domain reflectometry (TDR) is a technique used to test electrical interconnects and transmission lines in high speed circuitry (e.g. serial disk drive communication protocols, Ethernet cabling systems, etc.). Any changes in the impedance of the current path (transmission line) can be mapped, because these cause reflections at the interfaces between domains of differing impedance (as indicators of differences in dielectric constant of the medium surrounding the transmission line). The technique relies on variation in the dielectric relaxation of media in contact with the transmission line, and, furthermore, the location of discontinuities in the dielectric properties of the adjacent media can be determined. As such, simple sensing systems, which are directly amenable to remote sensing situations can be realized. This approach has been applied to a wide range of systems, although the primary application has been to soil samples, and evaluation of volumetric water content in these samples. It should be noted that frozen water in soils an electrolyte salt concentration in soils have been measured, as well. Furthermore, the sensors themselves (elements of a transmission line) are very inexpensive. Examples of recent applications of this technology to sensing (as opposed to testing) include measurement of resin flow in polymer curing applications¹, water and ice content in soil systems^{2,3,4}, and detection of ice, water and deicing solutions of aircraft wings and rotors.⁵ Indeed because of the ease with which dielectric relaxation measurements can be made over such a wide frequency range (1 MHz to 20 GHz), TDR has been applied to fundamental research involving the structure of water⁶ and the relaxation of water bound to silica gel.⁷

Like impedance spectroscopy, TDR allows one to measure dielectric relaxation, but at a much higher frequency and bandwidth. Furthermore, in principle, changes in the complex dielectric function of material near the sensing transmission line elements can be resolved in terms of the positional dependence along the length of the transmission line to a resolution of a centimeter or less.

The effective real part of the dielectric “constant” of water is approximately 80, while that of ice is 3. The TDR technique can also be employed to measure the conductivity of salt solutions, such as the deicing systems commonly in use.

The detailed the physics of TDR measurements cannot be presented in the framework of this report, so only a brief introduction will be given. The technique involves applying a very fast rise time (ps time frame) voltage pulse to one end of a transmission line. The pulse travels down the transmission line at a velocity nearing the speed of light, which depends on the dielectric properties of the medium surrounding the transmission line, according to:

$$v = c / \sqrt{\epsilon} = c / n$$

where, c is the velocity of light in vacuum, ϵ is the dielectric constant of the medium surrounding the transmission line and n is the complex refractive index of that medium.

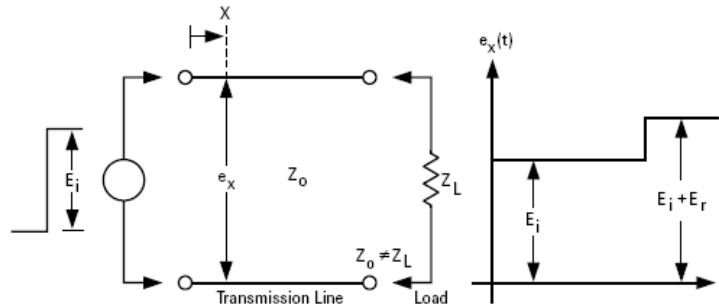


Figure 3.1. Voltage vs time at a point on an impedance mismatched transmission line driven with a step voltage of height E_i .

As depicted above, any point along or at the terminus of a transmission line where the impedance changes, due to a change in dielectric constant of the surrounding medium, a portion of the energy in the pulse is reflected back to the source. That portion of energy not reflected or adsorbed at a discontinuity continues down the line until it is either absorbed or reflected. The physical position of the discontinuity can be determined with appropriate calibration. For example, consider a segmented system as shown in the following figure:

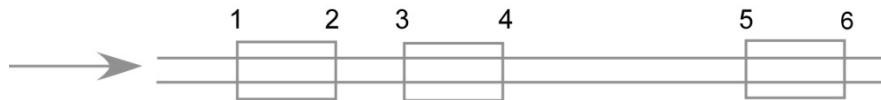


Figure 3.2. Transmission line with 6 dielectric discontinuities.

As the launched pulse encounters each dielectric discontinuity (points 1-6), a portion of the energy is reflected back to the source. In addition to determining the location of these dielectric discontinuities, a more detailed analysis of the differential complex impedance of that reflection can be made, and from this analysis the effective dielectric constant determined and attributed to materials for which the dielectric properties have been previously calibrated (e.g. water, ice, and electrolyte solutions).

Figure 3.3 shows the reflected pulse for a terminal sensing arrangement in which R and C represent the circuit equivalence impedances associated with the conductivity and dielectric loss associated with a salt solution. Here the solution properties of the electrolyte (real part of the dielectric constant and conductance) may be extracted for the measured values of R and C .

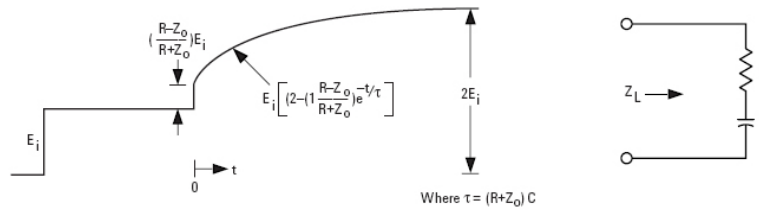


Figure 3.3. Idealized TDR trace for a series RC terminated transmission line.

Due to the significant difference in the real and imaginary components of the impedance of ice, water and deicing solutions, these boundaries are easily discerned.⁹ With respect to the spatial sensitivity and other design issues, reasonable care must be exercised in the physical and electrical design of the transmission line. Care must also be taken to impedance match the line to the source impedance of the TDR pulse generator, to preserve optimal sensitivity and spatial resolution. Given that transmission line theory is well established, such optimizations should be relatively straightforward. During the first year of this study the primary focus of the experimental work will be on the design of transmission lines in terms of geometry and materials employed, with consideration of segmented or continuous lengths of transmission lines also under consideration.

By analogy to the reported sensitivity to location and state of water on aircraft airfoil and airframe surfaces, we propose to examine the use of TDR to examine the state of water on various pavement and overlay surfaces.⁹ As in the case of the lower-frequency impedance measurements, various fixtures will be examined to evaluate optimal geometry and placement of the sensor (transmission) line relative to the surface under test. The effectiveness and tradeoffs of long runs of transmission line sensor (TLS) will also be examined, to ascertain whether or not arrays and networks can be used to map the state of water across large areas of roadbed or bridge deck surface. In principle a single TLS should be useful over a 150 m distance, so long as the dielectric in contact with it is not overly lossy, permitting spatial resolution of approximately 1 cm. One of the most promising aspects of this technology is the ability to sample various segments of a single transmission line, multiple transmission lines or a combination of both using a single set of TDR electronics in conjunction with commercially available network switches. As such, it is possible that commercially available TDR systems used for soil water analysis in agricultural applications (e.g. Trace system with a model 6020 multiplexer from Soilmoisture Equipment Corp., Santa Barbara, CA) could provide the electronics package for a 256 TLS array system covering an entire bridge, at a cost of approximately \$20K. Not only would this provide a significant advantage over light based technologies which sample a single spot, but at a considerably lower-cost per sensor site ($\$20K/256 = \$78/\text{sensor}$). Furthermore, many of these lower-cost systems are configurable for remote sensing applications (wireless modems, Bluetooth modules and battery powered electronics) which are particularly attractive attributes for this application.

Chapter 4

Development Focus and Sub-Tasks

Based on the proof of concept demonstrated in Phase I, further development towards a practicable application of TDR-based technology to the tasks at hand require continued refinement of all aspects of the system. These are broken down into those sub-tasks which are related to:

1. **Passive Sensor Development and Refinement:** Develop a wide range of sensor designs which vary geometric and materials considerations. Use simple software and correlation statistical indicators to assess the comparative efficacy of these.
2. **Acquisition and Testing of Electronics Components:** Evaluate commercially available TDR electronics components and acquisition software
3. **Software Development and Refinement**
4. **System Integration and Testing**

As such, each of these is treated in subsequent chapters.

Chapter 5

Sensor Test Stand

Test Stand. Temperature control experiments were conducted in an insulated container with both a model AC-194 peltier air cooler/heater and model CP-200TT cold plate made by TE Technology Inc. The air cooler/heater was mounted in the lid of the container and the cold plate up through the bottom of the container with the surface just above flush with the bottom interior surface. Power and temperature control was provided and accomplished by power sources and temperature controllers also from TE Technology Inc. A block diagram of the test system is shown in Figure 5.1. A metal pan used as a solution container was placed on top of the cold plate and held the solution that was being tested.

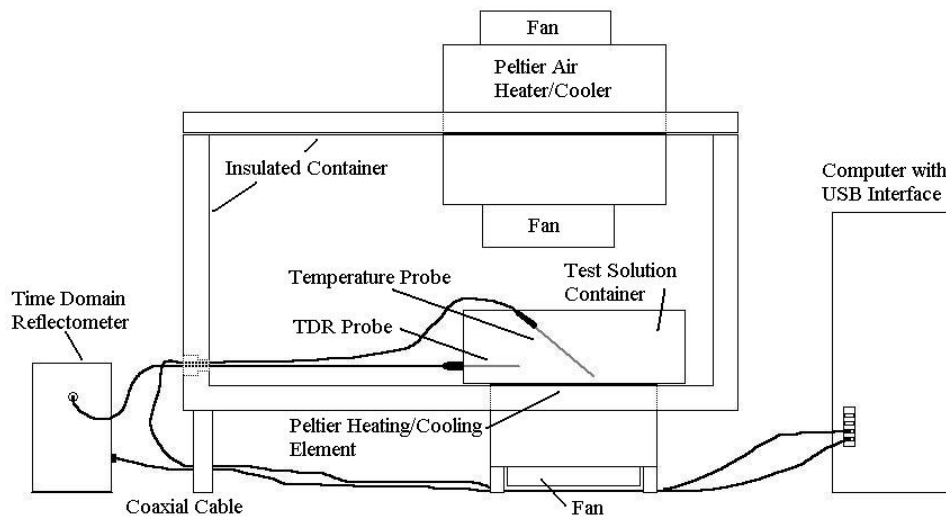


Figure 5.1. Block diagram of temperature controlled test cell.

The TDR probe was mounted to the pan through a hole cut in the side of it by piercing the three probe rods through a plastic rectangle and fixing the plastic to the side of the pan with silicone adhesive. A temperature probe purchased from Vernier was also placed in the solution container away from the TDR probes to provide temperature readings of the solution as it was cooled or heated. In all experiments involving liquid testing, 1L of the liquid was placed in the container at or slightly below room temperature. Tap water was used for testing and for making salt solutions. Diamond Crystal® Solar Salt of the extra course variety was used for salt solutions and has a purity of up to 99.6 percent. This salt and water were chosen because they are more likely

to be similar to the water and salt found on a bridge surface. Waveform spectra of air, water, and sodium chloride solutions were taken at room temperature and also as the test cell was being cooled. Temperatures well below freezing were obtainable when given proper time and dry ice was often placed around the metal pan to speed the process.

TDR test sensors were used to test responses from water, ice, air, and sodium chloride solutions. A large number of different configurations using a variety of conducting electrode material were fabricated and evaluated. These are discussed in Chapter 6, as these are one of the main considerations of this phase of the research project.

For simple sensor performance comparisons, software provided by Campbell Scientific[®] was used to collect the waveforms. It allowed continuous sampling and adequate control over averaging and resolution of the waveforms. The TDR data collected were saved as text files in ASCII format. This data was then available for analysis using either Microsoft Excel or programs written in LabVIEW (National Instruments). The software allowed the user to select a number of the text files to be used as standards in a database. Please see Chapter 8 for a discussion of advanced software and analysis development.

Chapter 6

Sensor Development and Refinement

Sensor Design Criteria. The general approach to sensor design was intuitive rather than being based on detailed electrodynamic modeling of the conducting elements and dielectric gap of the sensor. General aspects considered included the following:

1. Size.
2. Overall dimensionality: three dimensional vs planar structure.
3. Mechanical stability: ruggedness of the design with respect to anticipated environment when installed.
4. Drainage of liquids from the sensor elements, in particular the dielectric gap region.
5. Layout of the conductor pattern.
6. Relationship between the conducting or “hot” element vs a ground electrode.
7. Microscopic and macroscopic roughness of the conductor surfaces.
8. Chemical stability of the surfaces of the conducting elements.
9. Bare vs dielectric coating on the conducting elements.
10. Simplicity of fabrication.
11. Fabrication cost.

The electrode materials chosen were based on the ease of fabrication without concern for many of these, as a means of quickly exploring different electrode configurations without the expense of involving a machine shop in the fabrication of the device. As such most involved copper electrodes, but stainless steel, aluminum, nickel and nickel/silver alloys were employed in some designs. Wire, sheet and mesh configurations of conductor were evaluated. In many cases magnet wire (dielectric coated copper) was used. For dielectric insulators between the elements often epoxy potting compound was chosen, again for convenience. In each case fitting of 50 Ω BNC female connector to connect to the cable from the TDR source was required.

Shown below are some examples of the extremes in sensor design.

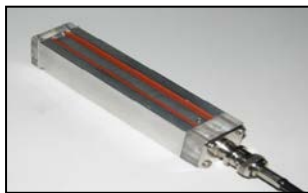


Figure 6.1. Machined Sensor, 0.25” square aluminum hot electrode and a 1.0” aluminum U-channel ground electrode with a 0.125” electrode gap.



Figure 6.2. Coaxial sensor constructed from stainless steel vacuum feedthroughs.

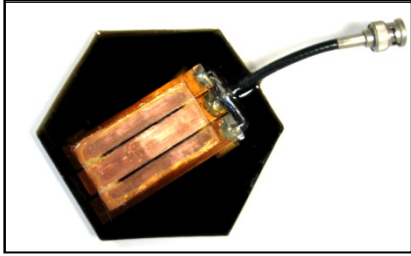


Figure 6.3. Linear sensor with small electrode gaps, 3"x0.5"x0.020" copper sheets with a 0.050" gap potted in a two part epoxy. Inner electrode is hot and outer two electrodes are ground.

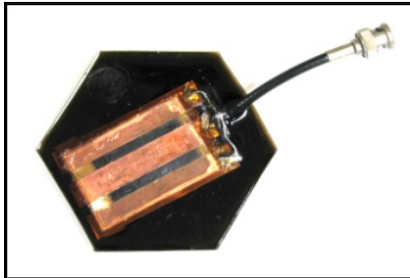


Figure 6.4. Linear sensor with large electrode gaps, 0.020"x0.5"x3" copper sheets with a 3/8" gap potted in a two part epoxy. Inner electrode is hot and outer two electrodes are ground.

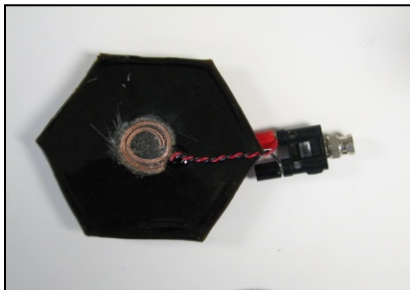


Figure 6.5. Jelly roll sensor, 0.020" copper sheet wound twice with a 1.0" outside diameter and potted in a two part epoxy. Hot and ground electrodes run side-by-side.

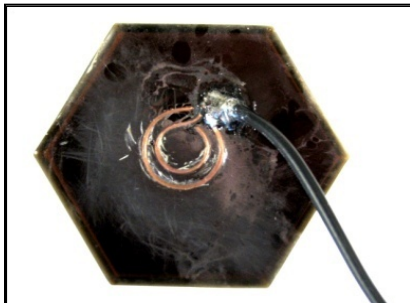


Figure 6.6. Open ring sensor with gaps in the diameter of the electrodes, 10 gauge copper wire with a ground electrode diameter of 1.125" and hot electrode diameter of 0.75" potted in a two part epoxy.

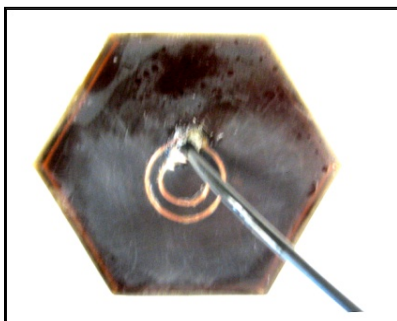


Figure 6.7. Closed rings sensor, 10 gauge copper wire with a ground electrode diameter of 1.125" and hot electrode diameter of 0.75" potted in a two part epoxy.

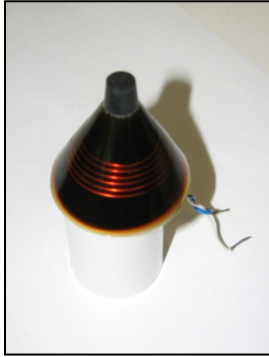


Figure 6.8. Cone sensor, 12 gauge magnet wire wound three times with a diameter decreasing from 1.5" to 1.0" potted in a two part epoxy. Hot and ground electrodes run side-by-side.

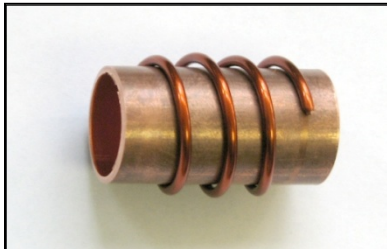


Figure 6.9. Spiral sensor, 12 gauge magnet wire hot electrode wound three times around a 7/8" diameter copper pipe ground electrode and potted in a two part epoxy. (Pictured before potting).

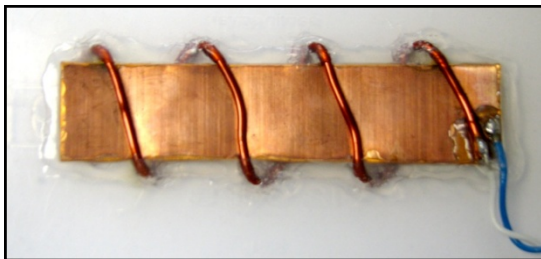


Figure 6.10. Spiral sensor, 12 gauge magnet wire wound three times around a 0.020"x1.0"x4.0" copper ground electrode.

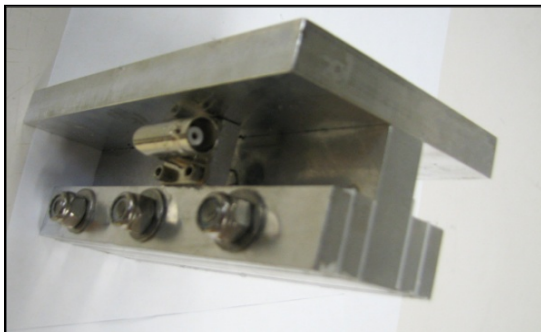


Figure 6.11. Machined aluminum sensor which allows for variable thicknesses of dielectric to be sandwiched between the electrodes. Teflon dielectric shown.



Figure 6.12. Single threaded sensor, 3.5" threaded stainless steel hot electrode in an aluminum U-channel ground. Packing tape used in-between the electrodes as the dielectric.

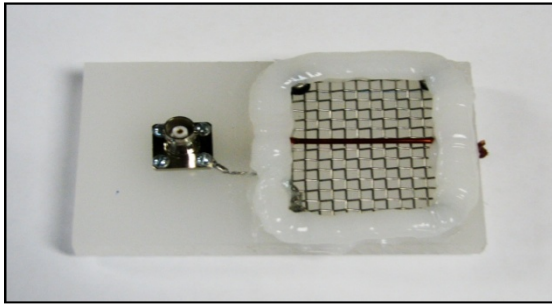


Figure 6.13. Mesh sensor, 3.0" long 12 gauge magnet wire over a 4x4 stainless steel mesh ground.

Sensor Performance. In general the best sensor designs were those which provided the largest differences between the TDR waveforms acquired for ice compared to air in contact with the electrode gap. This is a consequence of the similarity in the dielectric properties of these two media. Shown in Figure 6.14, is an example of a poorly performing sensor in which the signal processing software is severely challenged to distinguish between these responses.

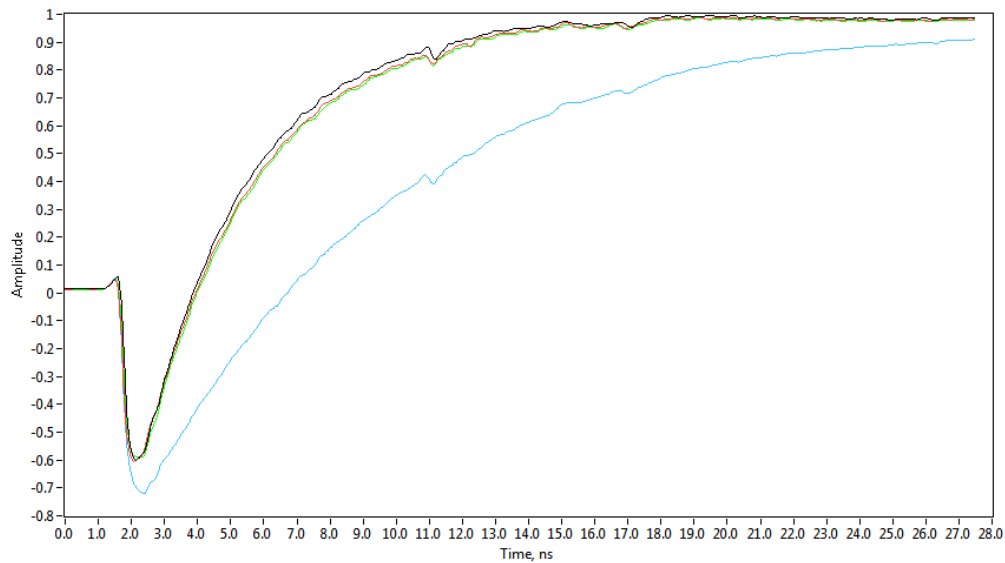


Figure 6.14. Example of poor raw data from a candidate sensor. Left to right: air, ice, frozen 0.1M NaCl, and water.

In contrast Figure 6.15 shows the case of a sensor with excellent differentiation between the responses to various media in the gap.

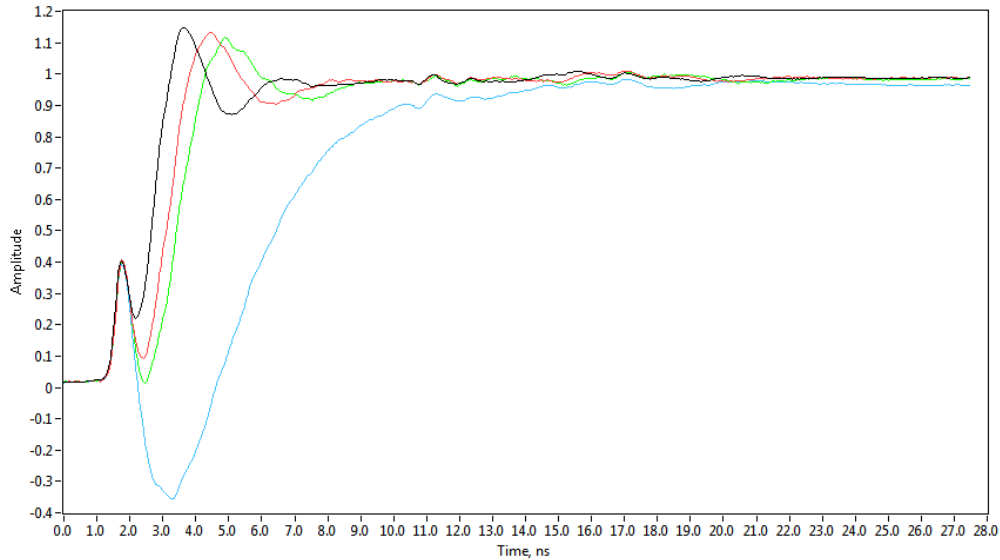


Figure 6.15. Example of raw data with high complexity and information content. Left to right: air, ice, frozen 0.1M NaCl, and water.

After applying the signal processing approach described in Chapter 8, the sensor performance can be quantified in terms of a set of values which compare the correlation coefficient returned when the calibrated response of known media (standard responses for a given sensor) is regressed against the sample response of an unknown medium in contact with that sensor. Values range between 0 and 1, and a perfect sensor would provide the following set of responses for the sensor challenged by ice, air and water unknowns:

Table 6.1. Ideal sensor response.

Unknown Medium	Correlation Coefficient		
	Regressed Against Ice	Regressed Against Air	Regressed Against Water
Ice	1.00	0.00	0.00
Air	0.00	1.00	0.00
Water	0.00	0.00	1.00

It should be noted that there are multiple criteria for success. High correlation coefficient for the correct response combined with low correlation coefficients for *all other media*.

As an example the following Figure and Table show results for the sensor shown in figure 6.2, above.

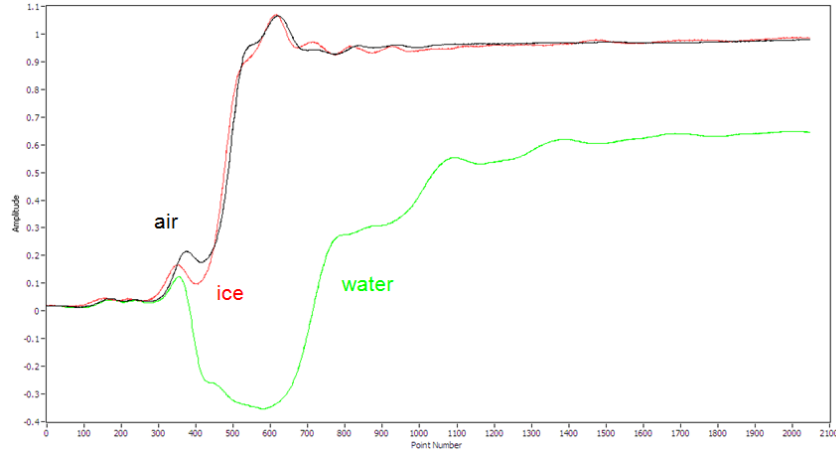


Figure 6.16. Raw responses for the sensor shown in Figure 6.2 for ice, air and water.

Table 6.2. Correlation coefficients for the sensor shown in Figure 6.2.

Unknown Medium	Correlation Coefficient		
	Regressed Against Ice	Regressed Against Air	Regressed Against Water
Ice	0.97	0.81	0.03
Air	0.96	0.98	0.04
Water	0.03	0.04	0.99

From these results it can be concluded that this is a bad design which should not be pursued further as ice-air differentiation is minimal. Although more sophisticated signal processing may improve the differentiation, other physical sensor designs must be considered as well.

Several general desirable design criteria emerged from the multitude of crude sensor mock-ups which were studied in this phase of the project:

1. The smaller the dielectric gap the better.
2. The smaller the electrode cross section the better.
3. The more convoluted or tortuous the electrode shape the better, as this introduces more “character” to the raw responses.
4. Sensors with coated electrodes (e.g. magnet wire which has a varnish coating on the copper wire) perform less well compared to their uncoated counterparts.
5. Corrugations in the electrode provide better responses than electrodes with smooth surfaces.
6. Electrodes fabricated from materials which do not corrode perform better than those whose surfaces accumulate dielectric oxide deposits. This is reflected in time-variance in the calibration sets.

These then are the criteria to be used for the next phase of sensor development.

Chapter 7

Acquisition and Testing of Commercial Electronic Components

After considerable research on the availability of commercial instrumentation to fulfill the needs of this project, it was decided to choose Campbell Scientific as the source for these electronics. Not only was the cost of these units found to be quite reasonable, but also the availability of data acquisition and data logging software to support these instruments obviated the need for the time required to develop these capabilities in-house. Furthermore, Campbell's experience and installation base suggested long-term availability and stability of their TDR platform due the company's acceptance among the agricultural and soil science communities. In addition, their equipment was found to be supported by various remote communication protocols so that. Looking ahead to future deployment, we could expect minimal delays in implementation of remote sensor stations such as rural bridges, etc., which are not supported by CAT-5 or optical cable connectivity, as could be expected for deployment on a bridge located on an interstate highway. Likewise, power for the electronics package would need to be supplied from batteries which could be recharged using solar panels. All of these criteria could be met using Campbell Scientific as a sole source supplier.

System Vision. Our vision for the ultimate deployment of a practicable system would involve the layout schematically depicted below.

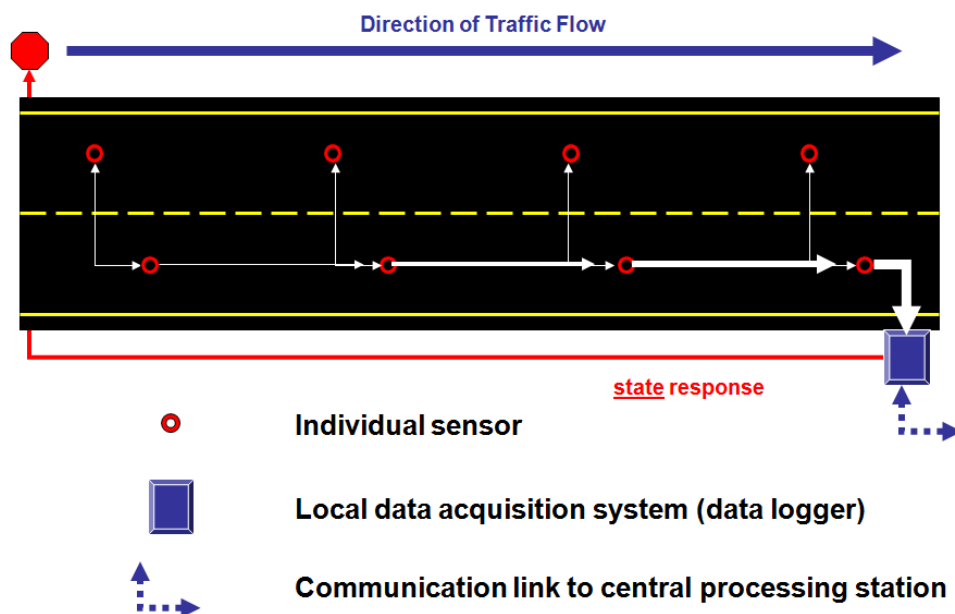


Figure 7.1. Schematic of a bridge deck installation at a remote location with 8 sensors deployed.

The system would have a local electronics package to acquire data from the sensor array in a multiplexed fashion and transmit these raw data to a central processing station which would support a large number of such installations in a given region. The central processing station would receive these data in real time and process the raw transients from the sensor array against

a bank of standards generated for calibration of each individual, specific sensor against the unknown media to be tested (e.g. air, ice, water, etc.). The software executing at the central processing station would then provide a single, binary output for each sensor or sensor array: alert or no alert with regard to potentially unsafe conditions. This information could then be sent back to the installation to activate signage warning motorists to the bridge deck condition, or alternatively notify maintenance personnel of a need to apply deicing chemicals or plow.

System Specification. While custom electronics could be designed and built to provide the requisite instrumentation package for a remote installation, for the sake of expediency commercial electronics provided by Campbell Scientific were chosen as discussed above. The overall package required included the following components:

1. Datalogger with remote telecom (wireless modem) capability.
2. Time domain reflectometer.
3. Multiplexer to allow for distributed sensor array (support for a minimum of 8 sensors), low contact impedance was deemed a crucial figure of merit to minimize corruption of the sensor excitation pulse generated by the Reflectometer.
4. Cell phone modem for remote communication (i.e. transmission of acquired data to central processing station, uploading of data logger programs, etc.).
5. Software to support datalogger, Reflectometer and multiplexer.
6. Solar panel and deep cycle batteries to provide power where it would be otherwise unavailable.
7. Weatherproof enclosure to house all electronics.

Commercial components Purchased and Their Costs. The following Campbell Scientific components were specified and ordered to provide a complete system:

1. CR1000-XT-SW-NC measurement and control datalogger	\$1520
2. TDR 100 time domain reflectometer	\$3600
3. SDMX50SP 50 ohm coax multiplexer	\$580
4. RAVEN XTV, Airlink CDMA cellular digital modem for Verizon systems, including antenna and mounting hardware kit	\$641
5. SP20, 20 watt solar panel	\$398
6. CH100-SW, 12 volt charger/regulator	\$178
7. BP12, 12 volt sealed rechargeable battery	\$110
8. Loggernet software	\$575
9. ENCTDR weatherproof enclosure	\$408
 Station cost	 \$8010

Chapter 8

Software Developments and Refinements

Optimization of Acquisition Parameters. When acquiring raw data (e.g. reflected TDR transients) from a candidate sensor, four parameters are important to optimize (averages, points, start, and length). Average input can vary from 1 to 128 averages and it is the number of separate waveforms that the TDR100 averages together to calculate the displayed waveform. Standard files were taken at 8, 16, 32, and 64 averages while keeping the other three parameters constant to test which value would lead to the greatest correlation between a sample file and a previously acquired standard. Diminishing returns were found after 16 averages. The number of points employed to represent the transient responses can vary from 2 to 2048 points and this parameter determines the data density of the acquired waveform. Standard files were taken with 256, 512, 1024, and 2048 points while keeping the other parameters constant. It was found that found after 512 points was optimum when correlating sensor calibration files with unknown sample files in real time. From these tests 16 averages and 512 points became the routine parameters for calibration and testing candidate sensors.

The delay times before the start of an acquisition cycle was optimized by gathering the waveform shortly before the first reflection from the sensor so that a baseline reference level could be included in the file. The length for the acquisition of each waveform was optimized by using a value that would allow the waveform voltage to come to approach a steady state value at the end of the data vector representing the transient response.

Analytical Software Development. For purposes of identifying unknown states of the sensor as compared to calibrated responses for known media (e.g. water vs air vs ice, etc.) various approaches were taken to optimize the differentiation between the waveforms of varying media for a given sensor, signal processing and sensor geometry. National Instruments' LabVIEW 2009 was used to develop a software package capable of comparing 'live' waveforms (samples) with a bank of standard calibration waveforms, while accurately determining the identity of the sample(s). This was accomplished by using relatively sophisticated regression methods to determine the correlation between each calibration standard and the sample(s) being considered. The identity of the standard with the highest correlation with the sample was then selected as the identity of the sample. This software was designed to use processing techniques intended to maximize differentiability among waveforms which contributed to the effectiveness of the software package.

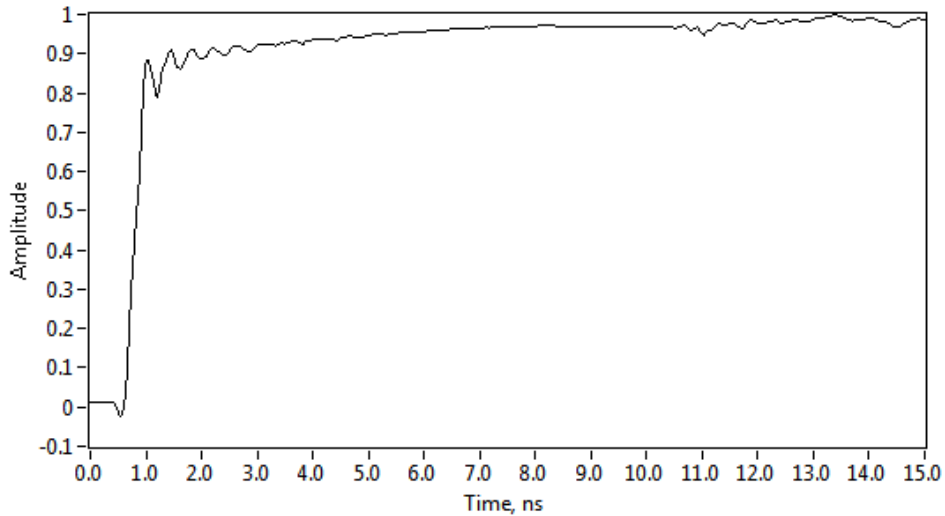


Figure 8.1. Raw data file taken with TDR 7.5cm probe in air.

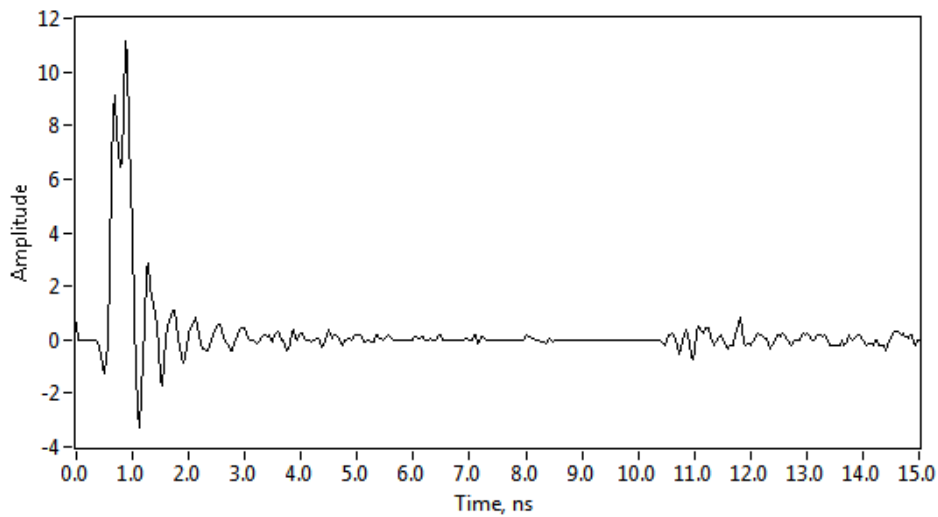


Figure 8.2. Raw derivative of Fig. 8.1 showing increased information content and complexity.

First, as shown in figs. 8.1 and 8.2, the software differentiated the calibration standard waveforms and the waveforms of the sample(s) being analyzed. This step increased the information content, or the complexity, of each waveform considerably, allowing for more precise differentiation between samples. Next, each derivative was digitally filtered to remove high-frequency noise using Savitzky-Golay smoothing (fig. 8.3), a widely used technique in which each point in the waveform was replaced with a point determined by a polynomial fit (of order k) of a interval width (number of points) on either side of the point to be replaced. The optimal polynomial order was determined to be 3rd order, and the number of side points 10 (21 point interval width).

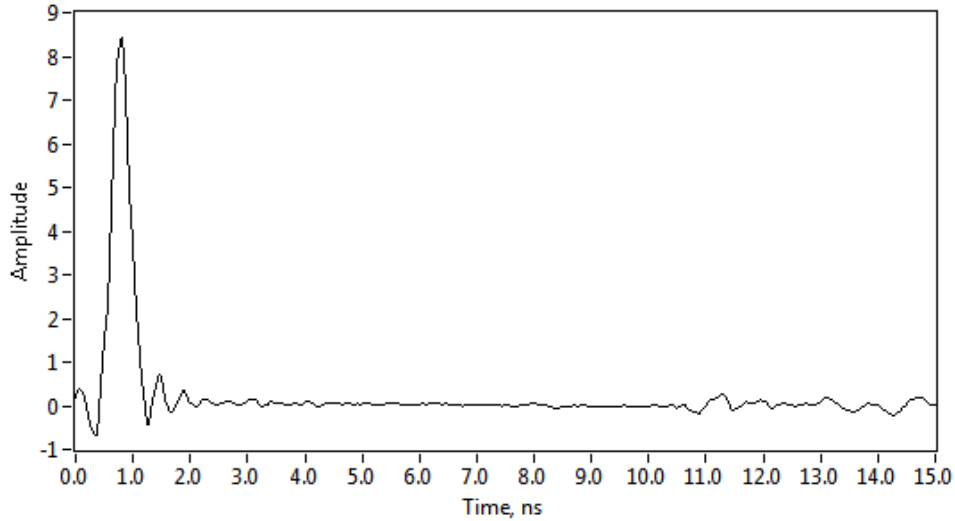


Figure 8.3. Savitzky-Golay smoothed derivative of Fig. 8.1.

Correction for Temperature Variations in Connecting Cables. It is important to note that the propagation rate of the signal along the transmission line from the TDR100 to the sensors may vary with temperature. This will be most pronounced for long cable runs between the TDR electronics and the sensor. As such there is an expectation of shifting of the starting point of the reflected pulse which requires a time-shift correction. In the context of this analysis system, this phenomenon manifested itself by shifting the collected waveform in the viewing time frame.

Two approaches may be taken to compensate for this time shift. First, the temperature of the transmission line can be monitored, and an appropriate correction applied. Alternatively, the start of the first reflection can be inferred from the shape of the acquired waveform. The solution implemented to solve this problem consisted of shifting the sample waveform before correlating it with each standard. This was accomplished without introducing error by using peak alignment as seen in the last step of the diagram below (Fig 8.4). The first major minimum of the sample waveform ('major' being defined by a threshold value set by the user) was aligned with the first major minimum of the standard calibration waveform and then regressed. The output value of this regression was deemed R^2_{der} , which ranged between 0 and 1.

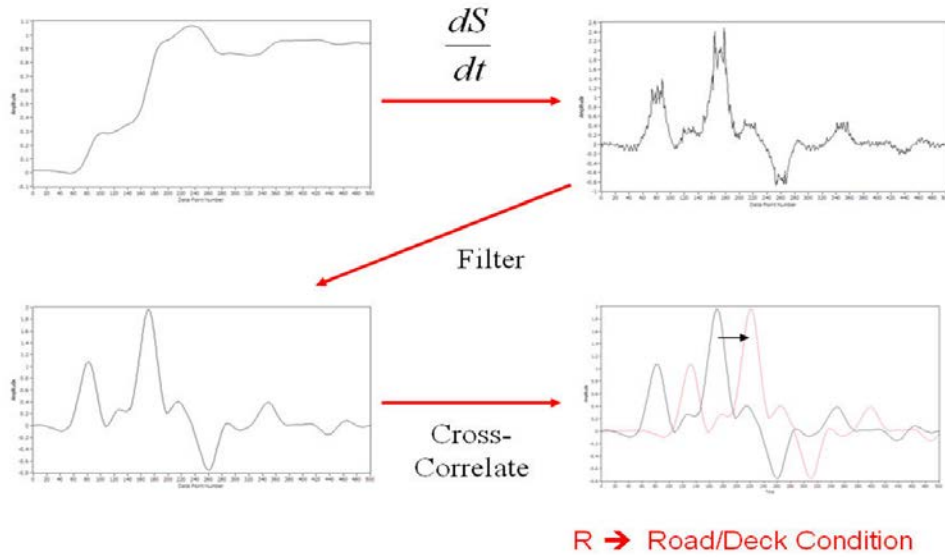


Figure 8.4. The waveform processing procedure implemented to optimize differentiability among waveforms, and the peak alignment technique used to overcome shifts induced by varying propagation rates due to changes in transmission line temperature.

Chapter 9 System Integration and Testing

A system consisting of the equipment describe in the preceding chapters was purchased and configured, including the use of wireless (cell phone data modem) data transfer to test the overall efficacy of the various components combined in a system which could be deployed after debugging and refinement. Testing included mock freeze-thaw cycles for a given sensor in initial contact with water. Shown below are the results in which the sensor in contact with water is cooled in the test chamber such that the water in contact with the sensor is frozen after about 1 min. The temperature is cycled back to room temperature, and the ice previously formed on the sensor is thawed completely at approximately 7 min. Clearly, success was achieved for this sensor as the transitions for the state changes are clearly indicated at these times. The “remote” unit was powered without the use of the solar panel-based power supply.

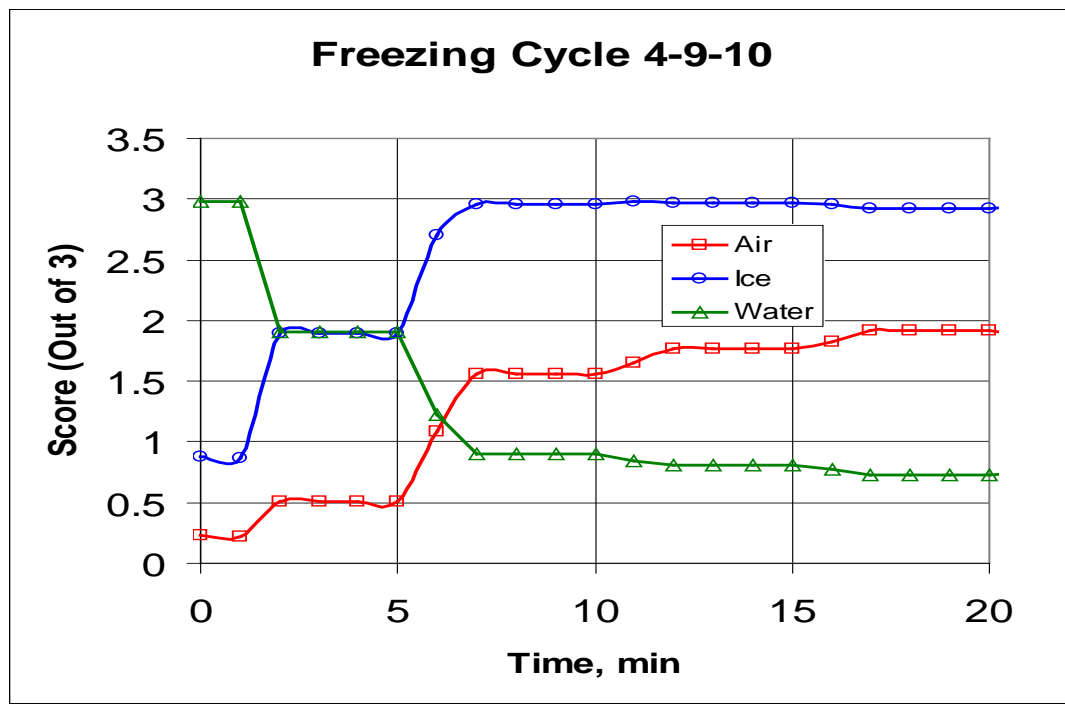


Figure 9.1. Freeze-thaw cycle for water from “remote” sensor located in the test stand. Raw data acquired by the datalogger transmitted to a “central” processing station running in-house developed software (written in LabVIEW).

Chapter 10

Suggestions for Future Work

The next phase of this project should focus on the following issues/goals:

1. Refinement of sensor design to optimize performance (air vs ice differentiation) and provide a mechanically robust configuration which is in a package amenable for installation in a bridge deck (as approved by MnDOT bridge engineers).
2. Refinement of data processing software to enhance differentiation between different media (including liquid and frozen electrolyte solutions to mimic deicing chemicals).
3. Actual deployment of a system onto a bridge deck after these refinements have been made for real world testing of a system.

References

- 1 D. Heider and A. Dominauskas, (2004) Composite Tech Brief, University of Delaware, Newark, DE (www.ccm.udel.edu).
- 2 C.-P. Lin, (2003) Frequency domain versus travel time analyses of TDR waveforms for soil moisture measurements, *Soil Sci. Soc. Am.*, 67, 720.
- 3 D.A. Robinson, S.B. Jones, J.M. Wraith, D. Or and S.P. Friedman, (2003) A Review of Advances in Dielectric and Electrical Conductivity Measurement in Soils Using Time Domain Reflectometry, *Vadose Zone J.*, 2, 444.
- 4 M.S. Seyfried and M.D. Murdock (1996) Calibration of time domain reflectometry for measurement of liquid water in frozen soils, *Soil Sci.*, 161, 87.
- 5 N.E. Yankielun, C.C. Ryerson and S.L. Jones (2002) Wide-Area Ice Detection Using Time Domain Reflectometry, US Army Corps of Engineers Tech. Rpt. ERDC/CRREL TR-02-15.
- 6 S. Mashimo, N. Miura and T. Umehara (1992) The structure of water determined by microwave dielectric study on water mixtures with glucose, polysaccharides, and L-ascorbic acid, *J. Chem. Phys.*, 97, 6759.
- 7 T. Sakamoto, H. Nakamura, H. Uedaira and A. Wada (1989), High-frequency dielectric relaxation of water bound to hydrophilic silica gels, *J. Phys. Chem.*, 93, 357.